CPS 2022 RFP – FINAL PROJECT REPORT

Project Title:
A viability assay for *Cyclospora* and its surrogates *Eimeria*

Project Period:
January 1, 2023 – December 31, 2024 (extended to January 31, 2025)

Principal Investigator:
Asis Khan, PhD
USDA ARS, Beltsville Agricultural Research Center (BARC)
Animal Parasitic Disease Laboratory
10300 Baltimore Avenue
Beltsville, MD 20705-2325
T: 202-236-0161
E: asis.khan@usda.gov

Co-Principal Investigators:
Benjamin M. Rosenthal, SD
USDA ARS, BARC
Beltsville, MD 20705-2325
T: 301-504-8301
E: benjamin.rosenthal@usda.gov

Jitender P. Dubey, MV Sc, PhD
USDA ARS, BARC
Beltsville, MD 20705-2325
T: 301-504-8128
E: jitender.dubey@usda.gov

Mark C. Jenkins, PhD
USDA ARS, BARC
Beltsville, MD 20705-2325
T: 301-504-8054
E: mark.jenkins@usda.gov

Objectives:

1. Adapt and validate sensitive biomarkers for risk assessments.
2. Develop quantitative viability assays for *Eimeria* and *Cyclospora*, using a droplet digital polymerase chain reaction (ddPCR) system and propidium monoazide (PMA) treatment.

Funding for this project was provided partly through the CPS Campaign for Research.

FINAL REPORT

Summary of Findings and Recommendations

This study addresses the challenge of reliably assessing *Cyclospora* viability to better understand and mitigate its health risks. Due to difficulties in propagating *Cyclospora*, reliable viability assessment tools are needed for growers and regulators. We sought to adapt methods developed for *Eimeria acervulina*, a close cousin, to assess *Cyclospora* viability. In *Eimeria*, dead oocysts were identified by their granular autofluorescence under ultraviolet light, a feature not seen in viable oocysts. This autofluorescence enabled sorting of live and dead oocysts using fluorescence-activated cell sorting. *In vivo* testing confirmed that only viable oocysts were infectious, while dead oocysts did not lead to shedding. A deep learning-based approach using high-resolution microscopic images was also employed to distinguish live and dead *Eimeria* oocysts, utilizing a convolutional neural network based on YOLOv7 architecture. The model achieved 99.1% precision in identifying oocyst viability, with over 95% accuracy in cross-species testing, demonstrating its applicability to other *Eimeria* species. Additionally, RNA sequencing of stored *E. acervulina* oocysts revealed age-related gene expression changes, particularly in heat shock proteins and ribosomal subunits. These findings provide insights into the biological processes underlying parasite senescence. By combining deep learning and transcriptomic data, this study presents a novel, cost-effective approach to assessing oocyst viability, enhancing the accuracy of risk assessments. This methodology offers regulatory authorities and growers a reliable tool for making informed decisions based on true parasite viability rather than detecting trace amounts of DNA, which may not pose an immediate threat. The approach holds promise for improving public health safety and parasite management.

Abstract

To effectively understand and mitigate the human health risks associated with *Cyclospora*, produce growers and regulators need reliable tools to assess not only the presence of the parasite but also its viability. The challenge in propagating *Cyclospora* hampers the ability to assess its viability. This study aimed to leverage knowledge gained from assessing the viability of *Eimeria* as a surrogate to develop viability tools for *Cyclospora*.

This study investigated the viability of *Eimeria acervulina* oocysts by examining morphological and molecular markers, with the aim of developing a rapid, reliable method to distinguish between viable and non-viable oocysts. High-resolution microscopic examination revealed that dead oocysts exhibited granular structures that autofluoresce under ultraviolet (UV) light, a characteristic not observed in viable oocysts. This autofluorescence was used as a basis for sorting live from dead oocysts using a fluorescence-activated cell sorting (FACS) cell sorter. In vivo challenge infections in chickens confirmed that only viable oocysts were infectious, while dead oocysts did not result in significant shedding. Additionally, a deep learning-based approach using high-resolution microscopic images was developed to distinguish between live and dead Eimeria oocysts. A deep convolutional neural network based on the YOLOv7 architecture was trained on these images, achieving a precision of 99.1% to differentiate between sporulated, unsporulated, and dead oocysts. The model also demonstrated over 95% accuracy in cross-species testing by successfully identifying oocyst viability in *E. maxima*.

Furthermore, we investigated the transcriptomic changes in *E. acervulina* oocysts that were stored at 4°C for extended periods using RNA sequencing (RNA-Seq). This analysis revealed significant age-related differential gene expression, with certain genes, such as heat shock proteins and ribosomal subunits, being upregulated as oocysts aged. These findings provide insight into the biological processes underlying parasite senescence.

The combination of deep learning techniques and transcriptomic data presents a novel, cost-effective, and rapid method for assessing oocyst viability. This approach holds significant potential for improving the accuracy of viability tools, allowing regulatory actions to be based on actual risk assessments rather than merely detecting trace amounts of parasite DNA that may not pose an immediate threat.

Background

Foodborne coccidia, including *Cyclospora cayetanensis*, pose significant threats to human health and the economy, especially through foodborne outbreaks and produce recalls [1]. *Cyclospora*, the cause of cyclosporiasis, is primarily associated with fresh produce imported from endemic regions such as Guatemala and Mexico [2-4]. The inability to propagate *Cyclospora* in culture or animal models complicates outbreak tracking and risk assessment, making it difficult to develop effective methods for detecting viable parasites. Recent studies have highlighted the genetic similarities between *Cyclospora* and *Eimeria* species, offering some insight into potential detection methods for *Cyclospora* [4, 5]. Current detection techniques, such as PCR and qRT-PCR, are commonly used to identify *Cyclospora* in food and environmental samples but cannot differentiate between viable and non-viable parasites. DNA can persist even after parasites die, leading to inflated risk assessments and undermining effective risk management strategies [6]. While RNA, which degrades more quickly than DNA, offers a better marker for live parasites, challenges remain in using RNA-based methods for large-scale testing, as variable gene expression complicates quantification, and RNA's fragile nature limits its use in real-world scenarios [6] [7].

To improve detection sensitivity, photochemical dyes like ethidium monoazide (EMA) and propidium monoazide (PMA) have been used to differentiate between live and dead parasites by exploiting their membrane integrity [8]. After entering the nonviable cells, PMA binds covalently to double-stranded DNA and, upon photolysis using bright white light, reacts strongly with hydrocarbons of the bound DNA, inducing permanent modification and rendering it inaccessible to DNA polymerase [8]. PMA with PCR or qPCR has been utilized extensively to differentiate live from the dead bacteria; however, these dyes face limitations in penetrating the tough, environmentally resistant outer layers of protozoan oocysts, such as those of *Cyclospora*.

Recently, we showed how long *Eimeria* species remained viable when stored at 4°C or 20°C temperatures, depending on the species [9]. Additionally, *in vitro*, excystation of *Eimeria* oocysts may not be a good indicator of oocyst viability [9]. *In vivo* methods to assess the viability of *Eimeria* oocysts are time-consuming and labor-intensive. The ability to quickly assess the viability of these oocysts would significantly enhance food safety regulations and epidemiological investigations, but no effective *in vivo* methods exist for assessing *Cyclospora* viability.

This study aims to develop a cost-effective, efficient approach for assessing parasite viability using phase contrast imaging and capturing autofluorescence differences using fluorescence-activated cell sorting (FACS). Another focus is on using deep convolutional neural networks (CNNs) to distinguish viable from non-viable *Eimeria* oocysts with simple white light microscopy. Additionally, we also hoped to identify biomarkers characteristic of dying and dead parasites and elucidate transcriptional pathways differentiating non-viable from viable oocysts. The study also tests the model's applicability across different *Eimeria* species, which are important in poultry production. The ultimate goal is to provide a practical solution for viability testing and foodborne pathogen risk mitigation. This research will help provide the industry, and regulators, with a rapid, sensitive, specific, and robust assay to diagnose parasite contamination and to test the presence of viable protozoan pathogens.

Research Methods and Results

Methods

1. **Parasites.** *E. acervulina* (APU1), *E. maxima* (APU1), and *E. tenella* (APU1) oocysts were propagated in Ross HR708 male broiler chicks every three months using a previously published method [10, 11]. After sporulation for 24 to 48 hours in a shaking water bath at 29°C, the oocysts were stored in 2.0% $K_2Cr_2O_7$ at 4°C. Oocysts were collected and examined at various time points (0 months, then every 4 months) by centrifugation, washing with PBS, and resuspending for microscopic examination and FACS.
2. **Microscopy.** Oocyst images were captured using different microscopy techniques. Phase contrast images were obtained with a Zeiss Axioskop 2 microscope. Differential interference contrast (DIC) images were captured using a Zeiss Axio Imager.M2 microscope. For high-resolution imaging, confocal microscopy with an LSM-710 system was used to analyze autofluorescence of *E. acervulina* oocyst membranes, with optical sectioning performed by imaging oocysts with Z-Stack slices in 1 µm increments.
3. **Fluorescence-Activated Cell Sorting (FACS).** *E. acervulina* oocysts were filtered and analyzed with a BD FACSAria™ Fusion Flow Cytometer using 405 nm (violet) and 488 nm (blue) lasers. The oocysts were categorized into populations based on autofluorescence intensity, with live oocysts (low fluorescence), dead oocysts (high fluorescence), and non-sporulated oocysts (third population). FACS analysis was performed using BD FACSDiva™ software to sort the oocysts into distinct categories for further study.
4. **Chicken Infection.** Two-week-old male Ross 708 chicks were orally infected with 1,000 FACS-sorted oocysts (live, dead, mixed, or unsorted). Three replicate groups per treatment were used. Fecal samples were collected five days post-infection, and oocysts were isolated by flotation in a saturated salt solution and washed with deionized water. Oocyst counts were performed using a McMaster chamber to calculate the number of oocysts excreted per chicken.
5. **Model Architecture and Training Details.** Utilizing the PyTorch library in Python, a classification model was built to assess the viability of *E. acervulina* and *E. maxima* oocysts. A YOLOv7-based classification model was developed to assess the viability of *E. acervulina* and *E. maxima* oocysts. The dataset was divided into 70% training, 15% validation, and 15% test datasets. Data augmentation, such as random flips and rotation, was applied during training to improve model generalization. The model was trained using a stochastic gradient descent optimizer on an NVIDIA A100 40GB GPU, with hyperparameters optimized using the validation dataset.
6. **Model Performance.** Model performance was evaluated using precision and recall, where precision is the proportion of true positives out of predicted positives, and recall is the proportion of true positives out of actual positives. These metrics were calculated to assess how well the model detected and classified the oocysts.
7. **Sample Preparation for RNA-Seq.** Oocysts were thawed and ground in TRIzol to extract RNA. The RNA was purified, quantified using a Qubit fluorometer, and its quality assessed by a Bioanalyzer. After DNase treatment to remove genomic DNA, RNA from multiple batches was pooled to ensure sufficient quantity for RNA-Seq assays. The pooled RNA was checked again for quality before sequencing.

8. **cDNA Library Construction and RNA-Seq.** cDNA libraries were constructed using the Illumina Stranded mRNA Prep kit [12], with size selection performed on some libraries to remove small adapter fragments. Libraries were sequenced using an Illumina MiSeq platform, and gene expression was quantified by calculating transcripts per million (TPM), which represents the relative abundance of each gene.
9. **Comparing Gene Expression Among Oocyst Cohorts.** Gene expression was analyzed across different age cohorts. Heatmaps were generated to visualize gene expression variance, and Pearson's correlation was used to assess the relationship between gene expression levels in different cohorts.
10. **Differential Gene Expression Through Time.** Differential gene expression analysis was performed using DESeq2 [13] to compare gene expression between 0-month and 30-month oocyst cohorts. Genes with significant changes (log2 fold change >1.5 or <−1.5, and adjusted p-value <0.05) were considered differentially expressed. Volcano plots were created to visualize the differential expression results.
11. **Homology Searching and Functional Genomics Analysis.** Gene functions were annotated using the *E. acervulina* reference strain from NCBI and ToxoDB. The Blast2GO tool was used to identify gene orthologs [14] and functional annotations. KEGG (Kyoto Encyclopedia of Genes and Genomes) pathway enrichment analysis helped identify biochemical pathways associated with differentially expressed genes [15].
12. **qPCR and Digital PCR to Validate RNA-Seq.** Quantitative PCR (qPCR) was used to validate RNA-Seq data for specific genes, including those with notable expression differences between the 0-month and 30-month cohorts. Digital PCR (ddPCR) was also employed to quantify gene expression in various cohorts, providing a more precise measurement of gene transcript levels.
13. **Ethics.** All animal experiments were conducted in compliance with the approved protocol from the Beltsville Agricultural Research Animal Use and Care Committee, USDA, ensuring ethical treatment of animals used in infection studies.

Results

1. **Identification of Granular Structures in Dead Oocysts of *Eimeria*** – We examined *E. acervulina* oocysts stored for 0–30 months, observing morphological differences between live and dead oocysts. Granular structures appeared in dead oocysts at 30 months, a feature absent in live oocysts (**Figure 1**). These structures were also observed in aging oocysts of *E. maxima* and *E. tenella*, suggesting a correlation between granule presence and parasite viability (**Figure 2**). These findings indicate that the granules may serve as markers for parasite viability, helping predict the infectivity of aged oocysts.

2. **Detection of Autofluorescence in Dead Oocysts –** Dead *E. acervulina* oocysts showed autofluorescent granular structures when illuminated with UV light (**Figure 3**). These structures were absent in live oocysts, providing a clear distinction based on fluorescence intensity. This difference in autofluorescence intensity can be used to separate live and dead oocysts, facilitating viability assessment.

3. **Fluorescence-Activated Cell Sorting (FACS) for Sorting Live and Dead Oocysts** – Using FACS, we successfully sorted live and dead *E. acervulina* oocysts based on autofluorescence intensity. Analysis of oocyst age cohorts revealed that 88.64% of 0-month oocysts were live, compared to only 15.67%

in 30-month oocysts. We then used FACS sorting to enumerate live and dead oocysts after mixing 0- and 30-month pools in ratios of 50:50, 25:75, and 75:25. The results correspond closely to expected ratios. Live parasites comprised, respectively, 49.69%, 38.16%, and 71.92% of these totals (**Figure 4**). Having established gating parameters from cohorts representing extremes of oocyst age, we then applied this tool to estimate the proportions of live, dead, and unsporulated parasites in cohorts of intermediate age (4, 8, 13, 18, 27, 29, and 30 months old oocysts) (**Figure 5**). These data indicated that more than 74% of *E. acervulina* oocysts, when stored at 4°C, remain living for up to 4 months. By months 8 and 13, more than 88% develop autofluorescent granular structures characteristic of dead oocysts (Figure 5). By 24 months, >95% are dead, and by 29 months, >98% are dead (Figure 5). FACS sorting demonstrated the ability to estimate live-to-dead ratios in mixed oocyst samples and identified a third population of unsporulated oocysts, which do not contribute to infection.

4. **In Vivo Assessment of Chicken Infectivity with Sorted Oocysts** – Chickens challenged with 1,000 sorted "dead" oocysts shed 100 times fewer oocysts than those exposed to "live" oocysts (**Table 1**). This confirmed that "dead" oocysts exhibit significantly reduced infectivity. The experiment also validated that sorting based on autofluorescence reduced infectivity in all cases, underscoring the biological relevance of the morphological distinctions made.

Conclusion of imaging and FACS study. Our rapid, sensitive, and robust assay holds promise for application to other species of coccidia, including those important to livestock and public health. Identifying distinguishing morphological features that distinguish dead from live parasites represents a welcome advance with several foreseeable applications, including the risk assessment in the context of produce safety. These data will benefit fresh produce growers and regulators seeking to safeguard public health and mitigate foodborne pathogens.

5. **Impact of Imaging Methods on Deep Learning-Based Detection of *E. acervulina* Oocysts** – We tested various imaging methods to train a YOLOv7 deep learning model to classify *E. acervulina* oocysts as live or dead. The model showed high precision and recall (above 87.4% and 77.1%, respectively) for all imaging methods, with phase contrast (PC) images outperforming differential interference contrast (DIC) and brightfield (BF) images (**Table 2**). PC imaging was selected for further evaluations due to its superior ability to visualize internal structures.

6. **Dataset Refinement for Enhanced Deep Learning Detection** – To improve deep learning performance, we included additional images of unsporulated oocysts in the training dataset. This refinement significantly improved model precision (from 92.1% to 94.6%) and recall (from 90.8% to 94.9%) (**Figure 6**). The enhanced dataset enabled the model to better differentiate between live, dead, and unsporulated oocysts.

7. **Cross-Species Applicability of the Oocyst Detection Model** – The detection model trained on *E. acervulina* oocysts successfully classified *E. tenella* oocysts with 99% precision but struggled with *E. maxima* due to the larger size of *E. maxima* oocysts (**Figure 7**). After fine-tuning the model with *E. maxima* images, the detection accuracy for this species improved to over 95%, demonstrating the model's potential for cross-species applicability (Figure 7).

Conclusion of the deep learning study. The deep learning-based detection model offers a cost-effective solution for assessing the viability of *Eimeria* oocysts. This model provides a practical alternative to existing methods like PCR and flow cytometry, offering reliable and accessible viability assessments for foodborne pathogens like *Cyclospora*.

8. **RNA-Seq of Aging *E. acervulina* Cohorts** – RNA sequencing of *E. acervulina* oocysts stored for up to 30 months revealed distinct gene expression changes as the oocysts aged. There was a decrease in transcriptomic correlation with age, with older cohorts exhibiting more similarities to the oldest group. This temporal shift in gene expression reflects the biological aging of *E. acervulina*, providing insights into the molecular basis of oocyst senescence.
9. **Expression Analysis Summary –** We analyzed ~6,900 *E. acervulina* transcripts using TPM to assess transcript abundance. Most genes contributed minimally, with 85% having <100 TPM, consistent with earlier findings. A few genes, such as EAH_00004110 and EAH_00015590, contributed disproportionately to the transcriptome (**Table 3**).
10. **Constitutive Gene Expression in Aged Oocysts –** In sporulating oocysts, 53 genes maintained >1,000 TPM throughout sporulation [16]. Thirty genes consistently expressed >1,000 TPM (ranging in mean TPM from 1,766 ± 588 (*EAH_00008670*) to 24,838 ± 14,275 (*EAH_00004110*)) across all cohorts (**Figure 8**). Notably, some genes had higher relative abundance in older oocysts (e.g., EAH_00004110), while others, like actin and profilin, were more abundant in fresh sporulated oocysts. This study identified a total of 60 genes that contributed >1,000 TPM from 0–30 months (Figure 8, Table 3). Several genes increased as oocysts aged, with some exceeding 60,000 TPM. Comparison with previous studies showed strong agreement in expression patterns.
11. **Functional Characterization of Genes –** The group of 30 constitutively expressed genes in common to unsporulated and sporulated oocysts largely overlap (~87%) the constitutively expressed genes we previously identified during sporulation (including *EAH_00004100*, *EAH_00004110*, resembling Cation-transporting ATPases in *Eimeria* spp.) and *EAH_00004780* and *EAH_00037050* (hypothetical proteins with resembling membrane proteins in other Apicomplexa) (Table 3). Thirty constitutively expressed genes were involved in housekeeping functions, with notable roles in actin dynamics, translation, and metabolism. Highly abundant genes like EAH_00002690 and EAH_00064490 were associated with motility and invasion.
12. **Variable Genes in Sporulated Oocysts –** Analysis of variance identified genes that increased in abundance as oocysts aged (**Figure 9**). While some genes contributed more early on, most were not highly abundant in older cohorts. Despite senescence, certain genes (*EAH_00007450, EAH_00046060, EAH_00049190, EAH_00053080*)) continued to dominate the transcript pool.
13. **Differentially Expressed Genes in Live vs. Dead Oocysts –** We identified genes with significant changes in abundance between 0- and 30-month-old oocysts, marking the transition from viability to non-viability. A total of 37% of the genes showed differential expression, with 1,086 up-regulated and 1,000 down-regulated (**Figure 10**).
14. **Major Transcripts Undergoing Differential Expression between 0 and 30 Months –** We identified 86 significantly differentially expressed genes (DEGs) between 0- and 30-month cohorts, all exceeding

1,000 TPM at month 0. Notably, only two of these genes (EAH_00007450 and EAH_00049190) appeared among the 50 most variably abundant genes. More than 25% (23 of 86) showed constitutive expression throughout the experiment. The majority of these genes (71/86, 82.6%) had higher expression at 0 months, with some showing more than a 6-fold (log2) increase, such as EAH_00059130 (heat shock protein 28) and EAH_00049190 (hypothetical protein). However, some genes, like EAH_00011300 and EAH_00059200, showed relatively small changes despite high expression at month 0. A gene of particular interest, EAH_000032920, showed a progressive decline in expression from 0 to 30 months and could serve as a potential marker for oocyst aging. In contrast, 15 genes contributed more at 30 months than at 0 months, with minimal changes (<2.8-fold log2). Notably, these genes, including EAH_00020540 (hypothetical protein) and EAH_00027050 (histone H2A), maintained high expression at 30 months. Functional categories among these upregulated genes include stress response (heat shock, peroxisomal catalase), metabolism (lactate dehydrogenase), and invasion-related processes (actin, myosin, SAGs), marking mature oocysts.

15. **Heat Shock Proteins and Aging –** We found 20 heat shock-related DEGs, with 80% upregulated at month 0 compared to month 30. These genes typically decreased as oocysts aged but showed elevated expression at intermediate months (8–13 months). Some genes (e.g., EAH_00007380) had decreased expression at 30 months but were minimally expressed at other time points. This suggests a role for heat shock proteins in senescence.

16. **Genes Downregulated in Aging Oocysts –** Some genes, such as EAH_00029830, EAH_00010660, and EAH_00020540, showed increased expression at 30 months. These included genes related to chromatin remodeling (EAH_00027050) and lipase activity (EAH_00010660). These findings highlight the stability of essential cellular processes (e.g., endomembrane systems, chromatin remodeling) in aging oocysts, while stress-related proteins declined.

17. **Genes with Increased Expression at 30 Months –** We identified 66 genes with >1,000 TPM at 30 months, showing a significant increase in relative abundance compared to month 0. These genes largely followed a consistent upward trend in expression, peaking at 30 months. Ribosomal protein genes (e.g., EAH_00003140, EAH_00007170) accounted for much of the increase, suggesting a shift toward fundamental cellular processes or ribosomal subunit preservation as mRNA degrades with aging.

18. **qPCR Validation and Digital PCR for Absolute Expression –** We validated RNA-Seq data using qPCR for selected genes (EAH_00004110, EAH_00020350, EAH_00049190), showing that qPCR estimates closely matched RNA-Seq results. As RNA quality deteriorated beyond 8 months, we turned to digital PCR for more accurate absolute expression profiles. These results revealed decreasing mRNA levels after 8 months, with detectable expression in older oocysts (25–30 months). Digital PCR confirmed expression trends consistent with RNA-Seq data, including the decline of EAH_00000650 and consistent upregulation of genes like EAH_00002690 and EAH_00021530 (**Figure 11**).

Conclusions of RNA-Seq study. Our findings suggest that aging oocysts exhibit a marked shift in gene expression, with genes involved in stress response, metabolism, and cellular repair becoming more prominent in aged oocysts, while others, particularly ribosomal proteins, increase in relative abundance. These data offer insights into the molecular aging of *Eimeria* oocysts, with potential applications in aging markers and viability assessments.

Outcomes and Accomplishments

- High-resolution microscopic examinations identified granular structures that are autofluorescent under UV exposure in dead oocysts. The presence of these granular structures only in dead parasites greatly increases overall autofluorescence intensity in dead oocysts compared to live oocysts. We harnessed this increased autofluorescence as a basis to sort live from dead oocysts using a FACS cell sorter. We validated the distinction between live and dead oocysts based on autofluorescent intensity by documenting infectivity in chickens using the former and minimal shedding with the latter. Our rapid, sensitive, and robust assay holds promise for application to other species of coccidia, including those important to livestock and public health.

- A deep learning model using YOLOv7 evaluated *E. acervulina* oocyst viability with phase-contrast images, achieving 99.1% precision and recall after dataset refinement. Cross-species testing with *E. maxima* showed over 95% accuracy. This approach enhances rapid assessment for vaccine development and coccidiosis management in poultry.

- We performed RNA sequencing (RNA-Seq) on *E. acervulina* oocysts to compare transcriptomes of freshly sporulated oocysts with those stored for 4–30 months. Despite decreased RNA integrity with age, we identified 60 constitutively expressed genes and confirmed 47 from a previous study. Over 81% of 6,867 genes showed differential expression, with 2,086 being significantly different. Fresh oocysts had 86 significant DEGs, while older ones had 66 upregulated genes, particularly those encoding ribosomal subunits. Key markers remained abundant as oocysts aged, with an increase in ribosomal RNA transcripts.

APPENDICES

Publications and Presentations

Publications:

- Valente MJ, Streett H, Turner R, O'Brien C, Fournet V, Jansen A, Dubey JP, Rosenthal BM, Jenkins M, and Khan A. 2025. Morphological and autofluorescence assessment of oocysts differentiate live from dead coccidian parasites. *International Journal for Parasitology* (in press). https://www.sciencedirect.com/science/article/pii/S0020751925000657

Publications (in progress):

- Park HW, Valente MJ, Fournet V, Rosenthal BM, Jenkins M, Khan A, and Nitin N, Deep learning-based detection and viability assessment of *Eimeria* oocysts. (Under preparation)
- Tucker MS, Hassan D, O'Brien CN, Yeager C, Khan A, Rosenthal BM, and Jenkins MC. Senescent *E. acervulina* oocysts maintain transcriptional activity during extended refrigerated storage and differentially express characteristic gene. (Under preparation)

Presentations:

- "A Viability Assay for *Cyclospora* and its Surrogates *Eimeria*" at CPS Research Symposium. Atlanta, Georgia, 2023; Denver, Colorado, 2024. (Poster presentations)
- "A Viability Assay for *Cyclospora* and its Surrogates *Eimeria*" at *Cyclospora* Task Force Webinar, 2023.
- "A Viability Assay for *Cyclospora* and its Surrogates *Eimeria*" at an international meeting "the first International *Cyclospora* Conference". Atlanta, Georgia, 2024.

Budget Summary

This project was awarded $215,765.00 in research funds, and all funds were spent except $13,067.56. We will spend the remaining funds to attend 2025 CPS Research Symposium. We appreciate CPS's flexibility and understanding as we endeavored to manage project funds to best ensure project success.

Figures 1–15 and Tables 1–3 (see below)

Figure 1. Comparative analysis of phase contrast images identified granular structures (black arrows) exclusive to aged oocysts of *E. acervulina*. A) Example phase contrast images of 4-month-old oocysts. B) Example phase contrast images of 30-month-old oocysts. Images were collected using an Axioskop 2 (Zeiss) microscope equipped with a UPlanFl 100x/1.3 oil ph3 phase contrast objective (Olympus). Scale bar = 10 μm.

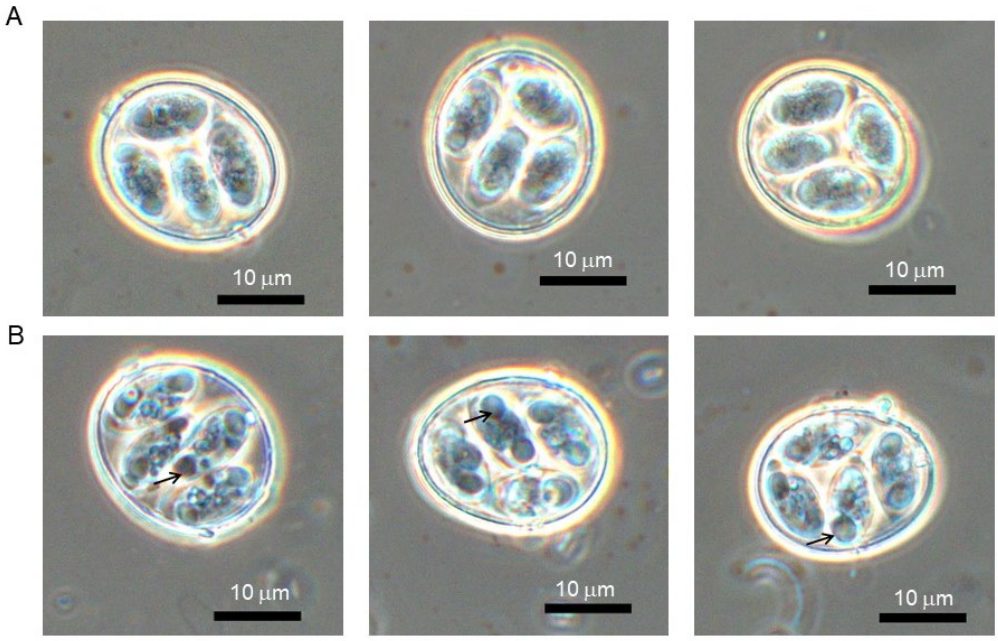

Figure 2. Phase contrast images showed the presence of granular structures (black arrows) in dead oocysts of *Eimeria maxima* (A = 4 months old; B = 30 months old) and *E. tenella* (C = 4 months old; D = 30 months old). Images were taken at 100x/1.3 oil ph3 phase contrast objective. Scale bar = 10 μm

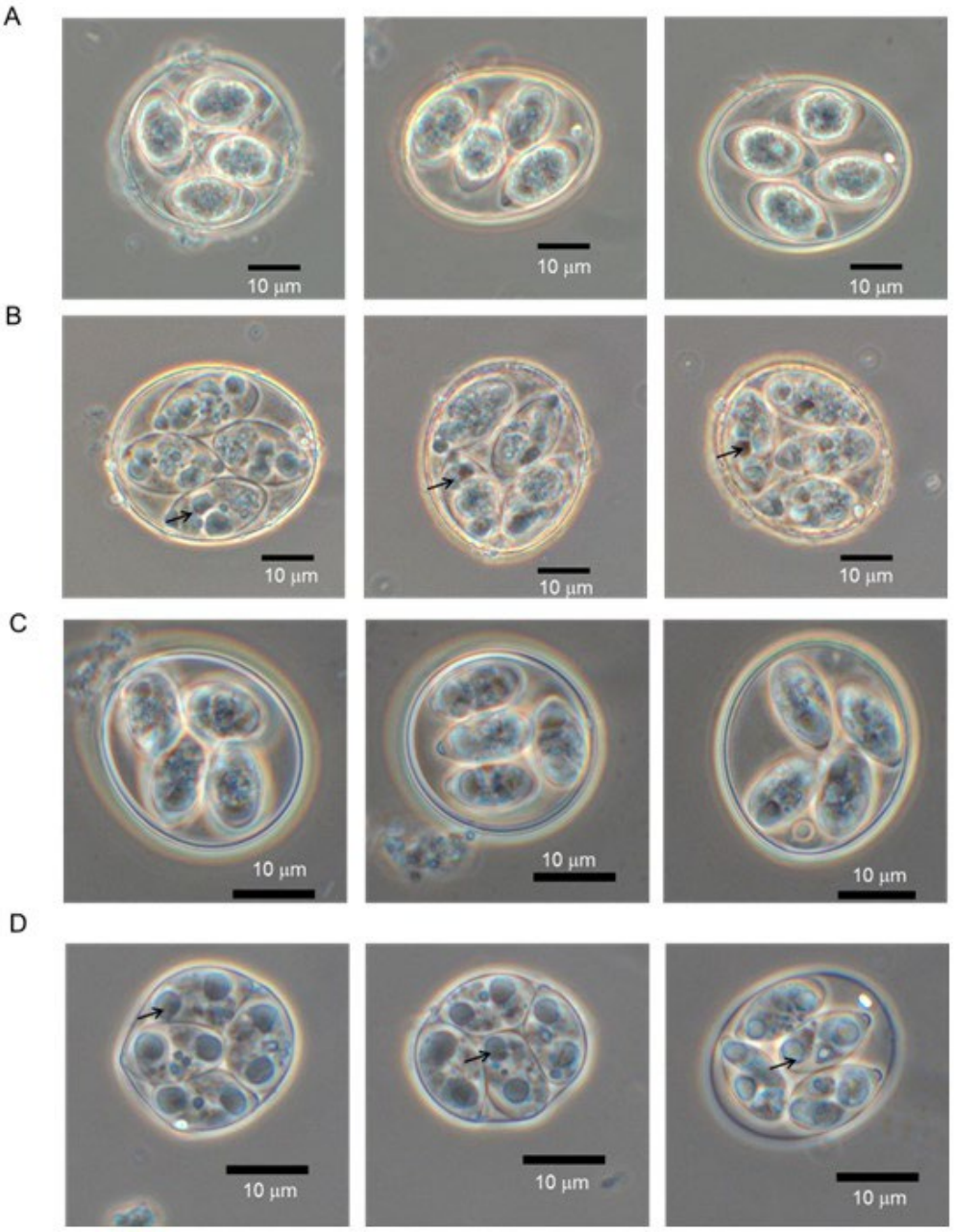

Figure 3. Pairs of confocal Z-Stack images depicted the autofluorescent property of the granular structures present in dead parasites, and the increased autofluorescence in dead oocysts. A, B, and C are differential interference contrast (DIC) images of live, dead, and a mixture of live and dead *E. acervulina* oocysts, respectively. D, E, and F depict these same oocysts employing excitation and emission wavelengths of 405 nm and 506, respectively. The filters used included a UV filter for oocyst autofluorescence, and the detection wavelength was maintained from 410 nm to 603 nm. White arrows indicate the autofluorescent granular structures. Scale bar = 10 μm.

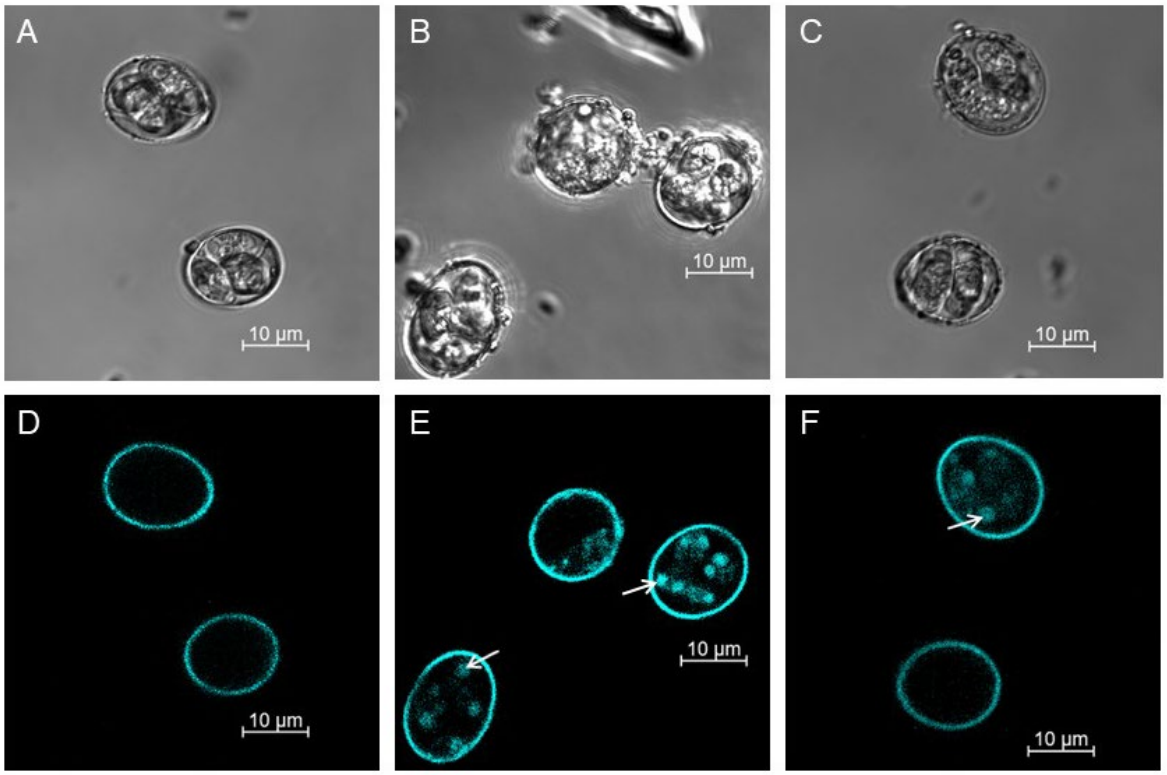

Figure 4. Live (4 months old) and dead oocysts (30 months old) were distinguished based on autofluorescence intensity differences using FACS. Oocyst populations were identified by autofluorescence emission when excited by 405 nm and 488 nm lasers and separated using filters for AmCyan and FITC fluorochromes. A) Tabulate representation of the FACS of defined ratios of 0- and 30-month-old cohorts. The P2 population represents live oocysts, whereas the P3 population represents dead oocysts. Ratio (%) Live:Dead column represents the mixing ratio of live and dead parasites. # Events indicate the counted raw number of oocysts by FACS. B) and C) Autofluorescence-restrictive gating strategy to identify the live, dead, and unsporulated oocysts. Fluorescence dot plots of FITC-A versus AmCyan-A (Panel B) and PerCP-Cy5-5-A versus AmCyan-A (Panel C) identified the live (purple, P6), dead (green, P7), and unsporulated (blue, P8) populations in mock mixtures of different ratios of live and dead oocysts (100:0, 0:100, 50:50, 75:25, and 25:75). D) Autofluorescence histograms represent the total count of live and dead oocysts present in mock populations. The population with lower autofluorescence intensity corresponds to live oocysts (P2) while the population with higher autofluorescence intensity corresponds to dead oocysts (P3).

A

Population	Ratio (%) Live: Dead	# Events	%parent
Live (P2)	100	6,220	88.64
Dead (P3)	0	797	11.36
Live (P2)	0	835	15.67
Dead (P3)	100	4,493	84.33
Live (P2)	50	2,442	49.69
Dead (P3)	50	2,472	50.31
Live (P2)	25	1,973	38.16
Dead (P3)	75	3,197	61.84
Live (P2)	75	4,420	71.92
Dead (P3)	25	1,726	28.08

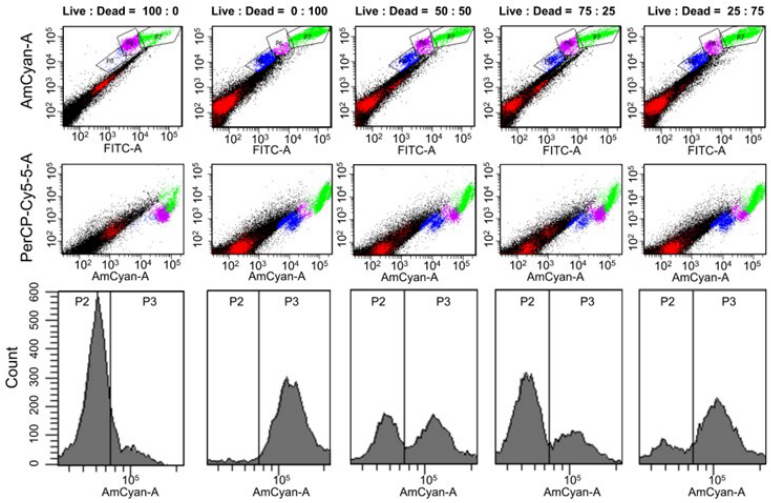

Figure 5. Counting live and dead oocysts present in the aged *E. acervulina* populations based on autofluorescent intensity using FACS. A) and B) represent the dot plots of FITC-A versus AmCyan-A, and PerCP-Cy5-5-A versus AmCyan-A, respectively, to estimate the live (purple, P6), dead (green, P7), and unsporulated (blue, P8) population in aged populations (4, 8, 13, 18, 27, 29, and 30 months old oocysts) as gated in figure 4. C) Histograms depict the frequency of live and dead oocysts present in the aged populations. Live and dead oocysts were identified using autofluorescence intensity based on the presence or absence of granular structures.

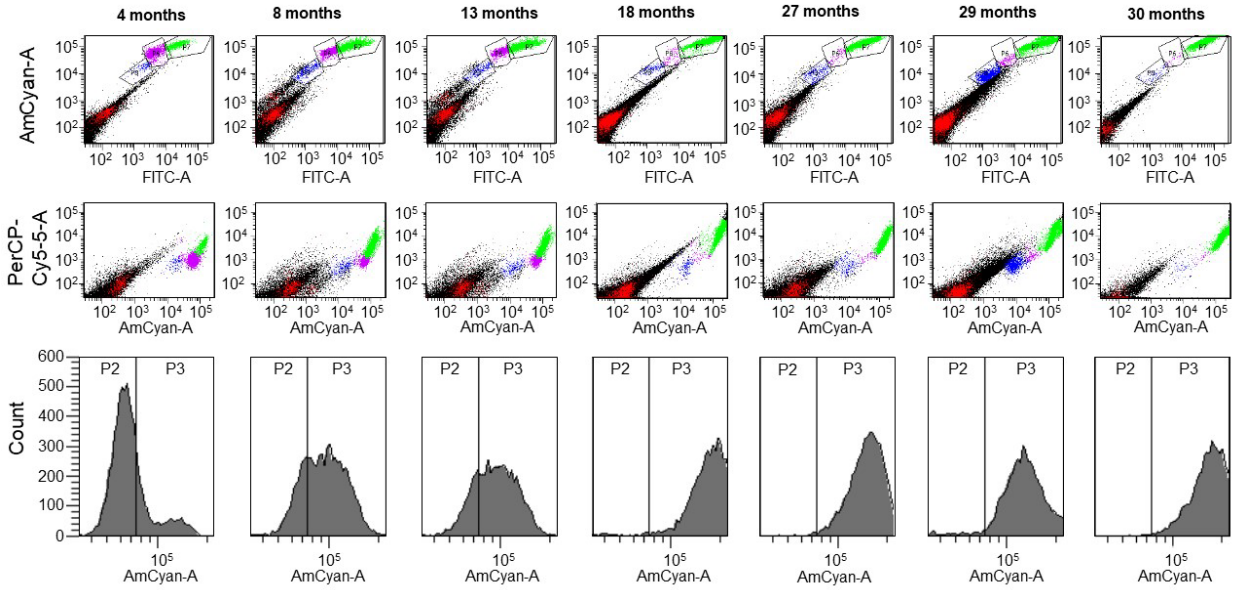

Figure 6. Detection of *Eimeria acervulina* oocysts using the deep convolutional neural networks and phase-contrast imaging: (a) 2-class classification and (b) 3-class classification.

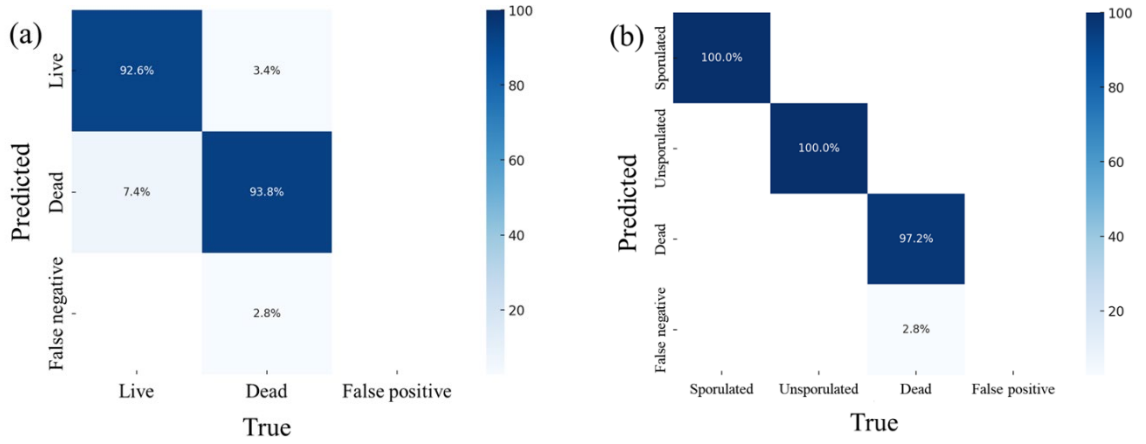

Figure 7. Detection of *Eimeria maxima* oocysts using the deep convolutional neural networks and phase-contrast imaging: (a) the model trained on *E. acervulina* and (b) the model fine-tuned on *E. maxima*.

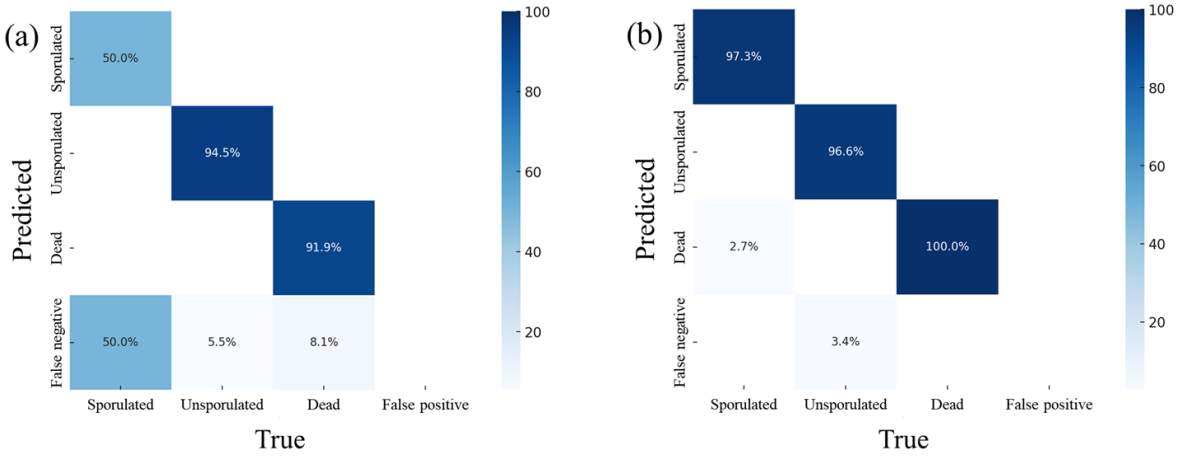

Figure 8. Comparison of mean TPM for constitutively expressed genes identified in aged cohorts of *E. acervulina* oocysts. A. For all cohorts (including unsporulated oocysts), 30 shared genes were identified; their expression was greatest in unsporulated oocysts (U). B. By excluding unsporulated oocysts, an additional 30 genes contributed >1,000 TPM throughout the 30 month study. TPM was elevated in cohorts stored at 4°C from 8-25 months.

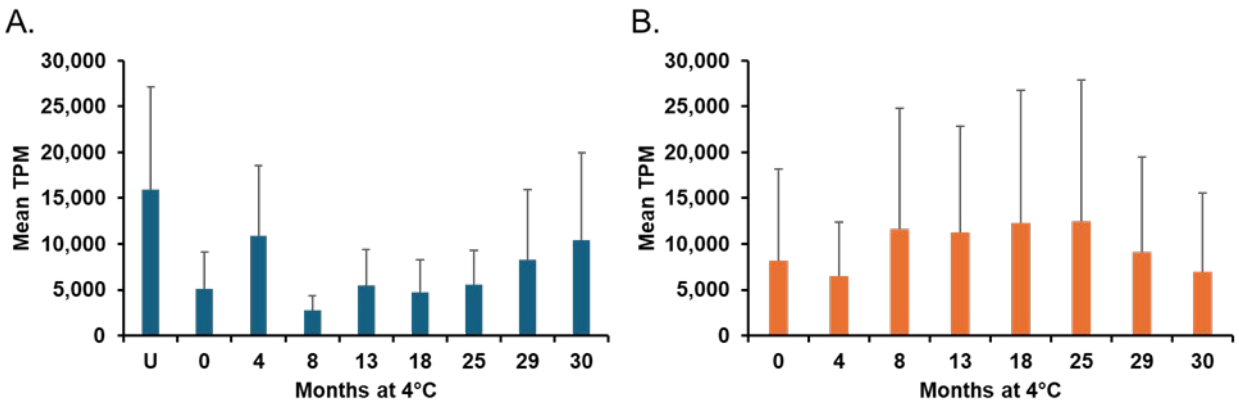

Figure 9. The 50 genes whose relative abundance changes most through time. Most of these genes increase in relative abundance as parasites age; fewer diminish in their relative abundance. Expression variation is displayed for $\log_2$ mean TPM.

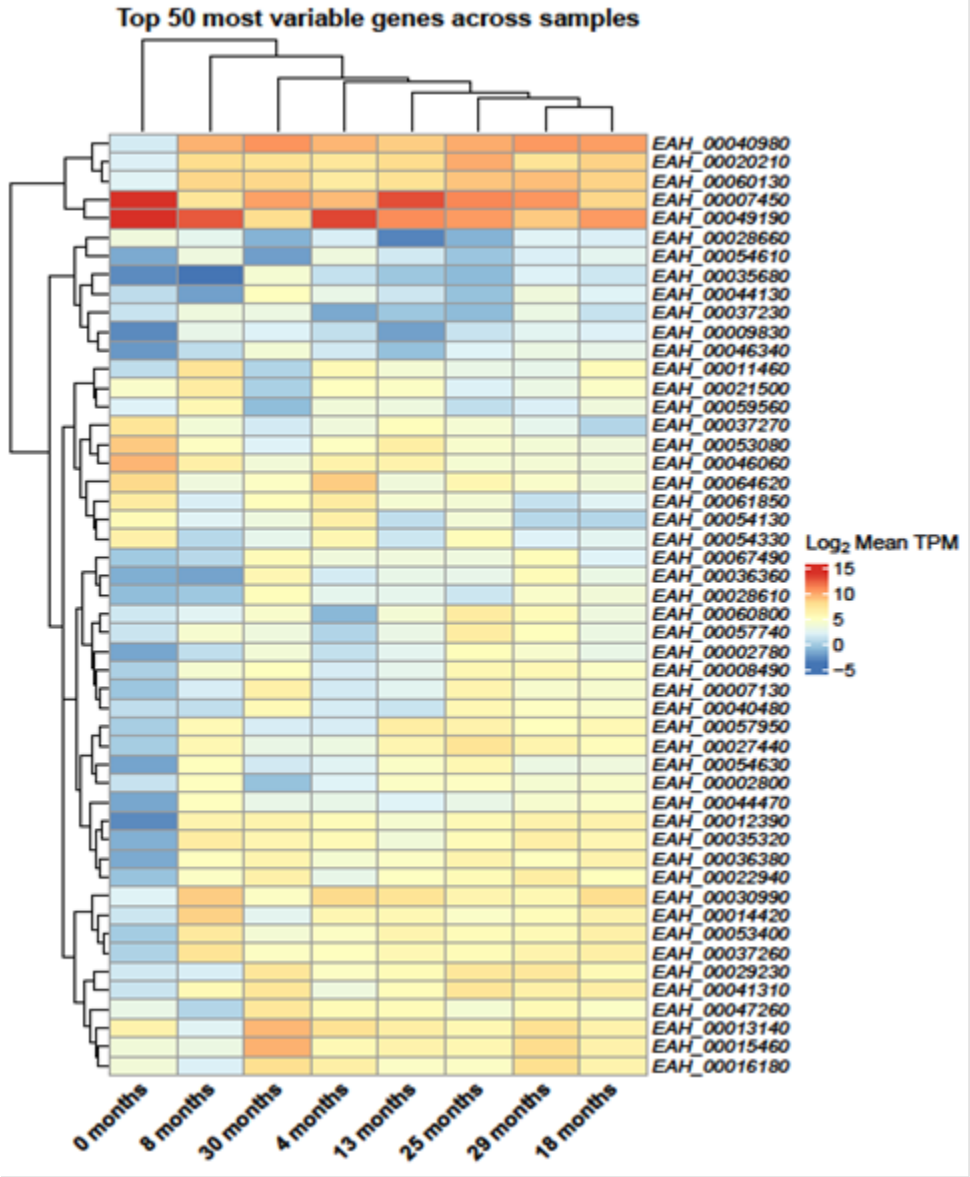

Figure 10. Major differential transcripts that markedly increase, or decrease, in relative abundance after *E. acervulina* oocysts underwent 30 months of storage (compared to those just sporulated). Of 5,622 genes whose transcript abundance sufficed to test for statistical significance in expression differences, 2,086 (37%) underwent a change of >1.5 or <-1.5 log_2 Fold Change (FC) with an adjusted p <0.05 (Adj. p-value). Of these,1,086 contributed more to the transcriptome at 0 months; 1,000 contributed more to the transcriptome after 30 months of storage.

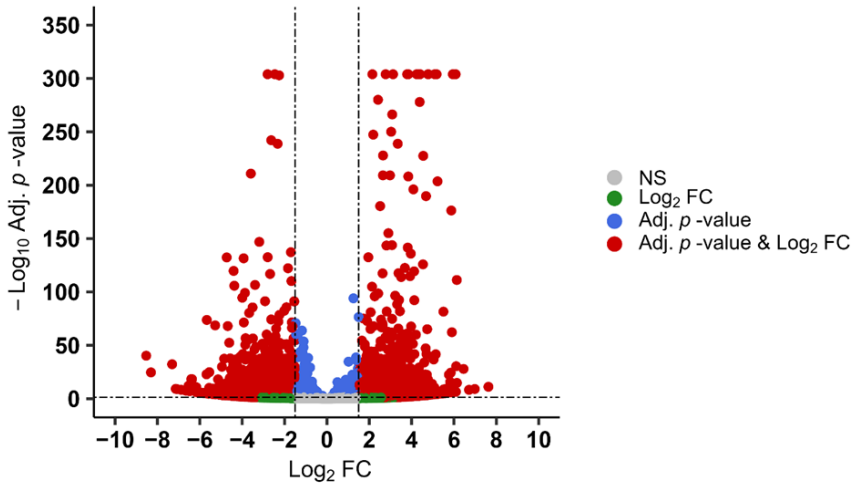

Figure 11. Digital RT-qPCR absolute expression estimation of genes in various aged cohorts. Genes *EAH_00000650*, *EAH_00002690, EAH_00004110*, *EAH_00007090*, *EAH_00010660*, and *EAH_00021530* are arranged in order from top to bottom, left to right. A. Digital qPCR data using first strand cDNA as template. Absolute expression is depicted for three replicates each of 0, 4, 8, 25, 29, and 30 months from left to right in each gene graph. B. Digital qPCR using double-stranded cDNA sequencing libraries. Absolute expression is depicted for three replicates each of 0, 25, 29, and 30 months from left to right in each gene graph. Note that 1-2 replicates for the 0 month sample did not amplify reliably but have been included in each gene graph.

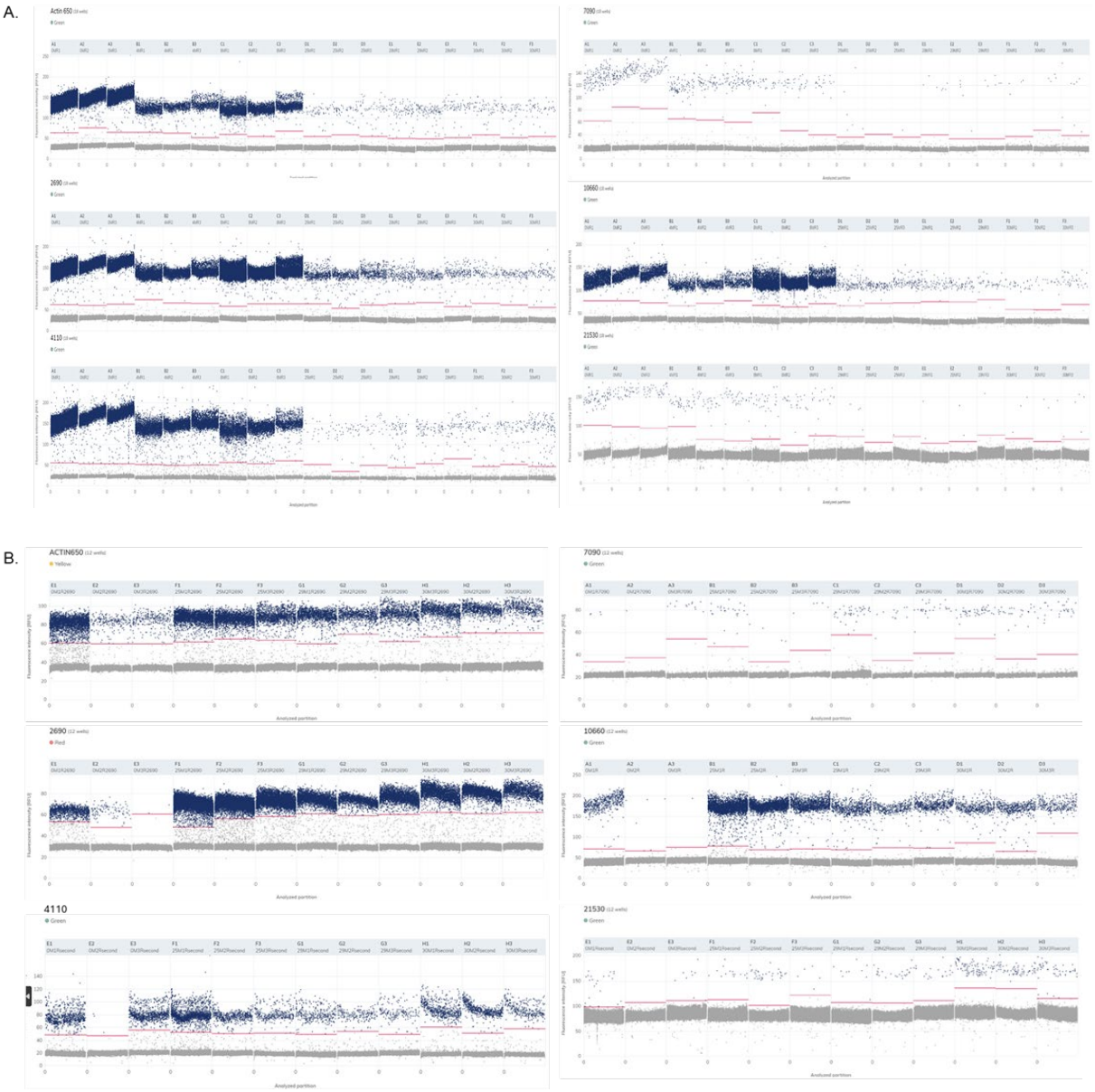

Table 1. Oocyst excretion from chickens challenged with FACS-sorted *E. acervulina* oocysts.

Group/Treatment	***Standard enumeration Total mean +/- SD oocysts (x10^6)***	***Coefficient of Variation***
Dead	0.17 ± 0.02	0.11
Live	19.3 ± 2.2	0.11
Dead + Live	16.5 ± 0.7	0.04
Control (unsorted)	46.2 ± 17.8	0.39

Table 2. Performance metrics for *Eimeria acervulina* oocyst detection using the deep convolutional neural networks with different imaging methods.

	Phase-contrast		Differential interference contrast		Brightfield	
	Precision	Recall	Precision	Recall	Precision	Recall
Live	93.1%	91.2%	84.1%	86.7%	87.9%	85.3%
Dead	91.2%	88.6%	92.3%	79.9%	87.0%	69.0%
Overall	92.1%	90.8%	88.2%	83.3%	87.4%	77.1%

Table 3. Summary and descriptive statistics of RNA-Seq data for different aged groups of *E. acervulina* oocysts

Months stored	Replicate*	Reads	Mapped Reads	Mapped reads (%)	Mean reads per triplicate	Reads SD per triplicate
	r1	1,697,936	1,541,043	90.8%		
Unsporulated	r2	2,369,306	2,158,594	91.1%		
	r3	1,621,188	1,475,095	91.0%	1,896,143	411,564
	r1	1,056,156	989,227	93.7%		
0	r2	1,428,778	1,338,083	93.7%		
	r3	1,922,402	1,800,033	93.6%	1,469,112	434,529
	r1	1,932,934	1,769,283	91.5%		
4	r2	1,577,872	1,447,357	91.7%		
	r3	1,154,220	1,059,317	91.8%	1,555,009	389,860
	r1	1,768,566	1,646,156	93.1%		
8	r2	1,063,808	986,234	92.7%		
	r3	1,441,558	1,336,908	92.7%	1,424,644	352,683
	r1	2,693,428	2,455,852	91.2%		
13	r2	2,000,036	1,776,589	88.8%		
	r3	2,016,682	1,826,678	90.6%	2,236,715	395,612
	r1	1,686,672	1,496,423	88.7%		
18	r2	1,423,034	1,298,344	91.2%		
	r3	2,069,778	1,602,892	77.4%	1,726,495	325,206
	r1	1,331,836	1,162,816	87.3%		
25	r2	1,622,294	1,407,671	86.8%		
	r3	1,858,120	1,583,341	85.2%	1,604,083	263,614
	r1	1,848,712	1,532,820	82.9%		
29	r2	2,321,444	1,935,628	83.4%		
	r3	1,741,658	1,547,683	88.9%	1,970,605	308,515
	r1	1,803,484	1,451,531	80.5%		
30	r2	2,296,274	1,817,005	79.1%		
	r3	1,400,300	1,083,828	77.4%	1,833,353	448,733
	Total	47,148,476	41,526,431			
	Mean	1,746,240	1,538,016	88.4%		
	Median	1,741,658	1,532,820	90.8%		
	SD	401,958	345,411	5.09%		

*RNA-Seq was performed on three technical replicates (designated r1, r2, r3) from each group

References:

1. Dixon, B., et al., *Detection of Cyclospora, Cryptosporidium, and Giardia in ready-to-eat packaged leafy greens in Ontario, Canada.* J Food Prot, 2013. **76**(2): p. 307-13.
2. Dubey, J.P., et al., *Endogenous Developmental Cycle of the Human Coccidian Cyclospora cayetanensis.* J Parasitol, 2020. **106**(2): p. 295-307.
3. Giangaspero, A. and R.B. Gasser, *Human cyclosporiasis.* Lancet Infect Dis, 2019. **19**(7): p. e226-e236.
4. Dubey, J.P., A. Khan, and B.M. Rosenthal, *Life Cycle and Transmission of Cyclospora cayetanensis: Knowns and unknowns.* Microorganisms, 2022. **10**(1): p. 118.
5. Tang, K., et al., *Genetic similarities between Cyclospora cayetanensis and cecum-infecting avian Eimeria spp. in apicoplast and mitochondrial genomes.* Parasit Vectors, 2015. **8**: p. 358.
6. Foddai, A.C.G. and I.R. Grant, *Methods for detection of viable foodborne pathogens: current state-of-art and future prospects.* Appl Microbiol Biotechnol, 2020. **104**(10): p. 4281-4288.
7. Shock, J.L., K.F. Fischer, and J.L. DeRisi, *Whole-genome analysis of mRNA decay in Plasmodium falciparum reveals a global lengthening of mRNA half-life during the intra-erythrocytic development cycle.* Genome Biol, 2007. **8**(7): p. R134.
8. Nocker, A., et al., *Use of propidium monoazide for live/dead distinction in microbial ecology.* Appl Environ Microbiol, 2007. **73**(16): p. 5111-7.
9. Jenkins, M.C., et al., *Relationship between Eimeria oocyst infectivity for chickens and in vitro excystation of E. acervulina, E. maxima, and E. tenella oocyst during long-term storage.* Poult Sci, 2023. **102**(12): p. 103133.
10. Ryley, J.F., et al., *Methods in coccidiosis research: Separation of oocysts from faeces.* Parasitology, 1976. **73**(3): p. 311-326.
11. Proszkowiec-Weglarz, M., et al., *Research Note: Effect of butyric acid glycerol esters on ileal and cecal mucosal and luminal microbiota in chickens challenged with Eimeria maxima.* Poult Sci, 2020. **99**(10): p. 5143-5148.
12. Tucker, M.S., et al., *RNA-Seq of Phenotypically Distinct Eimeria maxima Strains Reveals Coordinated and Contrasting Maturation and Shared Sporogonic Biomarkers with Eimeria acervulina.* Pathogens, 2023. **13**(1).
13. Love, M.I., W. Huber, and S. Anders, *Moderated estimation of fold change and dispersion for RNA-seq data with DESeq2.* Genome Biol, 2014. **15**(12): p. 550.
14. Gotz, S., et al., *High-throughput functional annotation and data mining with the Blast2GO suite.* Nucleic Acids Res, 2008. **36**(10): p. 3420-35.
15. Kanehisa, M. and Y. Sato, *KEGG Mapper for inferring cellular functions from protein sequences.* Protein Sci, 2020. **29**(1): p. 28-35.
16. Tucker, M.S., et al., *Dynamically expressed genes provide candidate viability biomarkers in a model coccidian.* PLoS One, 2021. **16**(10): p. e0258157.